THE PENNSYLVANIA STATE UNIVERSITY
SCHREYER HONORS COLLEGE

DEPARTMENT OF AEROSPACE ENGINEERING

AN EFFICIENT CFD APPROACH FOR CO-AXIAL ROTOR SIMULATIONS

JASON CORNELIUS
SUMMER 2018

A thesis submitted
in partial fulfillment
of the requirements for a
baccalaureate degree in
Aerospace Engineering
with honors in
Aerospace Engineering.

Reviewed and approved* by the following:

Sven Schmitz
Associate Professor of Aerospace Engineering
Thesis Supervisor

George Lesieutre
Professor of Aerospace Engineering
Honors Adviser

* Signatures are on file in the Schreyer Honors College.

ABSTRACT

The advent of small-scale multicopter aircraft including quad- and octocopter configurations has opened the door to cost-effective vertical flight technology. These aircraft are intended to be used in applications such as public transportation, recreational products, commercial tools, military technologies, and even extra-terrestrial planetary exploration. As the demand for these aircraft continues to rise, analysis capabilities for their design and performance prediction become increasingly useful. The complex problem involving rotor-rotor interactions calls for high-fidelity prediction tools, but conventional approaches with these tools have immense computational demand. In this work, a computational fluid dynamics model is developed to analyze a co-axial configuration and is compared to conventional results. The methodology, benchmarking process, and preliminary results indicate that the modeling approach, which reduces the computational cost by more than two orders-of-magnitude over the conventional solution method, has potential for future analyses to support design.

TABLE OF CONTENTS

LIST OF FIGURES

LIST OF TABLES

NOMENCLATURE

AOA	Angle of Attack	degrees
C_D	Vehicle/Blade Drag Coefficient	NA
C_d	Airfoil Drag Coefficient	NA
C_L	Blade Lift Coefficient	NA
C_l	Airfoil Lift Coefficient	NA
C_p	Airfoil Pressure Coefficient	NA
P	Reference Pressure	Pa
M	Mach number	NA
Re	Reynolds Number	NA
t	Time	s
x, y, z	coordinate system	m
x-axis	Stream wise positive	m
y-axis	Upward positive	m
z-axis	Span-wise positive	m
ρ	Density	kg/m^3
ν	Kinematic Viscosity	m^2/s
μ	Dynamic Viscosity	$kg*s/m^2$
p	Static pressure	N/m^2

ABBREVIATIONS

2D	Two-Dimensional
3D	Three-Dimensional
BL	Boundary Layer
CAD	Computer Aided Design
CFD	Computational Fluid Dynamics
Gb	Gigabytes
NACA	National Advisory Committee for Aeronautics
NS	Navier-Stokes
RAM	Random Access Memory
RANS	Reynolds-Averaged Navier-Stokes
SA	Spalart-Allmaras Turbulence Model
UAS	Unmanned Aerial Systems
VTOL	Vertical Take-Off and Landing

ACKNOWLEDGEMENTS

I would like to thank Dr. Sven Schmitz for first getting me involved in this research endeavor and giving his time to advise me along the way. Dr. Michael Kinzel, who first brought the mixing plane approach to my attention and assisted me throughout, as well as my lab mates Dr. Adam Lavely, Dr. Bernardo Vieira, Regis Thedin, Ethan Corle, and Amandeep Premi who were all instrumental in my success with developing the computational model presented. I'll also take the opportunity to thank Dr. George Lesieutre, Dr. Susan Stewart, Professor Rick Auhl, Amy Custer, and Kirk Heller of the Aerospace Department for their continued support and guidance over the years.

There were also a few folks within the broader College of Engineering who helped me immensely along the way. I credit much of my success at Penn State to a great personal friend of mine, Dr. Xinli Wu, whose mentorship has pushed me to be the very best I can be in all aspects of life. His travel-based study abroad course, "Impact of Culture on Engineering in China," first stirred my interest in developing a global perspective, which has flourished into several trips abroad to multiple countries. My involvement in the College of Engineering Research Initiative's (CERI) Research Experience for Undergraduates (REU) program with program leaders Erin Hostetler and Cynthia Reed was also a key driver early on in the work I've completed.

Three additional highly influential mentors, who no doubt guided me at different stages toward a research career in vertical lift, are Dr. Edward Smith of Penn State, Dr. Albert Brand of Bell Helicopter, and Dr. William Warmbrodt of the NASA Ames Research Center. I consider all three personal mentors and have only the utmost appreciation for their guidance.

I would also like to thank the folks involved in the 2018 Mid-East Regional AHS Robert L. Lichten competition for their feedback to help improve the scope and presentation of this work. Lastly, I would like to thank all my friends and family for their encouragement throughout my educational pursuits. The level of support has been nothing short of extraordinary.

"I come as one, but I stand as 10,000." – Maya Angelou

There are countless more people that have helped me at one point or another along this journey that is still moving with great speed. Although I can't list them all, their influence has nonetheless helped me move closer to my goals, and I am deeply grateful for it.

Chapter 1

Introduction and Background

Small-scale multicopter aircraft are continually becoming more popular in many aspects of society, and their usefulness stretches far beyond a commercial product. The increasing demand for these aircraft comes along with an increasing need to understand how they operate so as to improve their efficiency and performance. A large set of wind-tunnel based studies have been carried out at the NASA Ames Research Center among others, to increase the knowledge of these aircraft (Ref. 1-2). Prior work has also applied state-of-the-art computational analysis techniques based on computational fluid dynamics (CFD) to advanced vertical-flight aircraft design and analysis tools (Ref. 3-6). Such analyses, however, have a large computational cost associated with them that is not ideal for design.

The present research effort involves the development of a tool for analysis and optimization of multicopter aircraft. The driving purpose of this research effort aims to optimize the Dragonfly aircraft concept, Ref. 7, which is a multicopter with the goal of exploring Saturn's largest, methane-rich moon, Titan. The project is being funded through the NASA Frontiers program, which is supporting exploration and scientific study of the solar system. Dragonfly was selected as one of the two projects for the final competition. The project is lead by the John Hopkins Applied Physics Laboratory (JHAPL) in collaboration with the Pennsylvania State University Vertical Lift Research Center of Excellence (VLRCOE).

The full mission profile has been developed as part of the proposal and includes detailed plans to launch the Dragonfly aircraft via rocket to Titan on an approximate 9-year journey through the solar system. The aircraft will enter the atmosphere within a heat-shield enforced aeroshell, be slowed by parachutes that are jettisoned once speeds in which the aircraft can fly are reached, and land using its own devices. The capability for Vertical Take-Off and Landing (VTOL) will allow the Dragonfly aircraft to explore Titan's mid-latitude dune fields. The aircraft will be equipped with scientific instrumentation so as to gather data on Titan and create new knowledge on pre-biotic chemistry.

There is much fundamental research to be conducted before the aircraft can be sent on its mission to explore. The highly complex rotor-rotor interaction problem and a truly unique operational environment calls for a high-fidelity prediction tool to ensure mission success. The creation and validation of a CFD multicopter Unmanned Aerial System (UAS) model is presented. The project objectives focus on efficiently simulating the vehicle's flight. To this end, a novel rotorcraft CFD approach is applied and explored. The research has developed a high-fidelity, time-efficient, approach for optimization of multicopter aircraft.

Figure 1 shows a rendering of the Dragonfly concept. With an atmosphere different from Earth, a high-fidelity analysis tool was needed to aid in the design process. While developing the CFD model, a novel approach was explored and applied to a co-axial rotor. Table 1 shows a comparison of atmospheric properties for Earth and Titan.

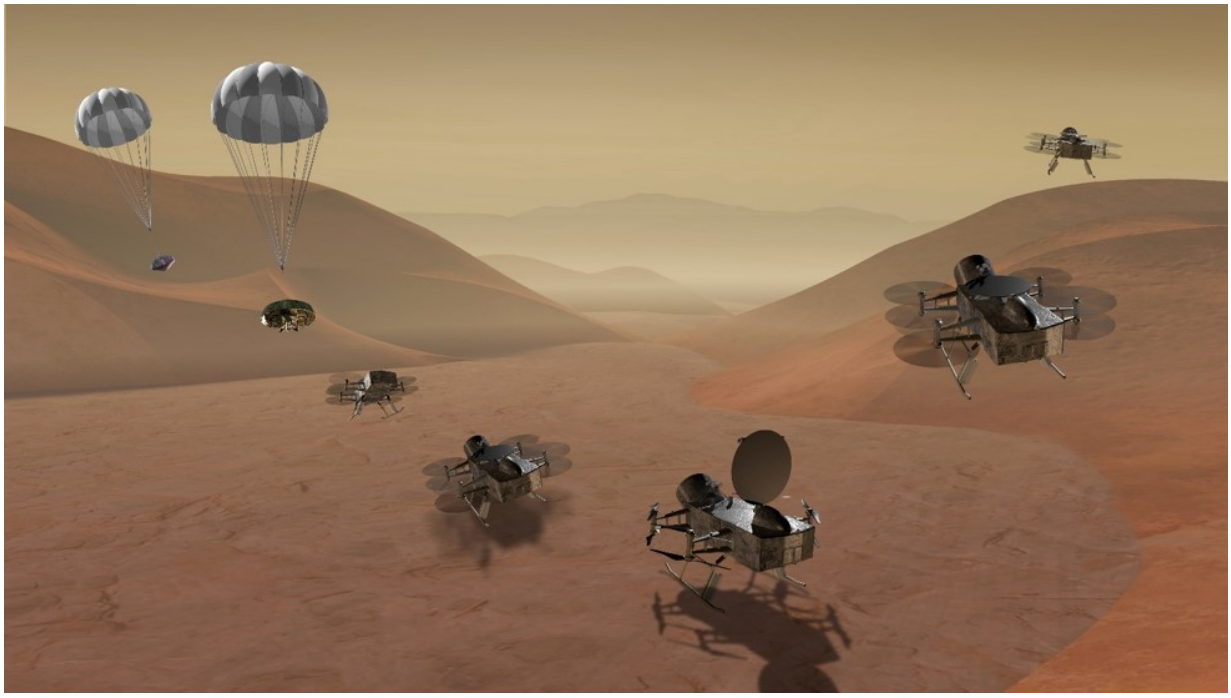

Figure 1. Dragonfly Aircraft Concept – Applied Physics Laboratory, John Hopkins University Ref. 7

Table 1. Atmospheric Conditions on Titan and Earth

Atmospheric Variable	Titan	Earth	Titan/Earth
Density, ρ (kg/m^3)	5.4	1.225	4.41
Dynamic Viscosity, μ (kg/ms)	$6.7x10^{-6}$	$1.8x10^{-5}$	0.37
Kinematic Viscosity, $nu = \mu/\rho$ (m^2/s)	$1.24x10^{-6}$	$1.5x10^{-5}$	0.08
Reference Pressure, P (Pa)	146,086	101,325	1.44
Speed of Sound, a (m/s)	195	330	0.59
Gravitational Acceleration, g (m/s^2)	1.35	9.81	0.14

The new high-fidelity, three-dimensional, CFD model, which is found to be efficient with respect to conventional methods, has been created within the toolset of Star-CCM+ (Ref. 8). In this effort, a mixing-plane approach, a method common in turbomachinery applications, is

proposed for application to co-axial rotors in hover. The simulation incorporates periodic boundaries that nearly halves the cell count in the context of a Reynolds-Averaged Navier-Stokes (RANS) CFD model and enables the usage of steady algorithms.

Objectives

The objectives of the research presented herein were to accomplish the following:

1. Develop a computational fluid dynamics approach to optimize multicopter aircraft.
2. Validate the model with theoretical methods.
3. Incorporate methods to reduce the computational demand.
4. Efficiently simulate hover of a co-axial rotor.

The present paper is outlined following the statement of objectives above. The paper initiates with a discussion of the proposed mixing-plane computational approach in the context of various conventional computational technologies relevant to rotorcraft. The CFD model is then evaluated and benchmarked using aerodynamics predictions for an airfoil, a semi-span wing, and a rotor blade. The model is then extended to hover conditions with the mixing-plane approach for single and co-axial rotor systems. Additionally, the same condition is also evaluated using a conventional time-accurate model. Comparing results between the present model approach and the time-accurate model characterizes the novel method with respect to accuracy and computational time. Results indicate the present approach has significant computational savings at a small cost to accuracy, which may lead to a CFD method better suited for design in hover conditions.

Chapter 2

Computational Methods

CFD Software and Computational Resources

The commercial CFD code, Star-CCM+, is used in this research for the model development and simulation. The software package contains the entire workflow from creating the baseline geometry all the way through visualizing the results. Based on user experience, the SolidWorks computer aided design (CAD) program was also used to create some of the geometry. Figure 2 shows the Star-CCM+ graphical user interface.

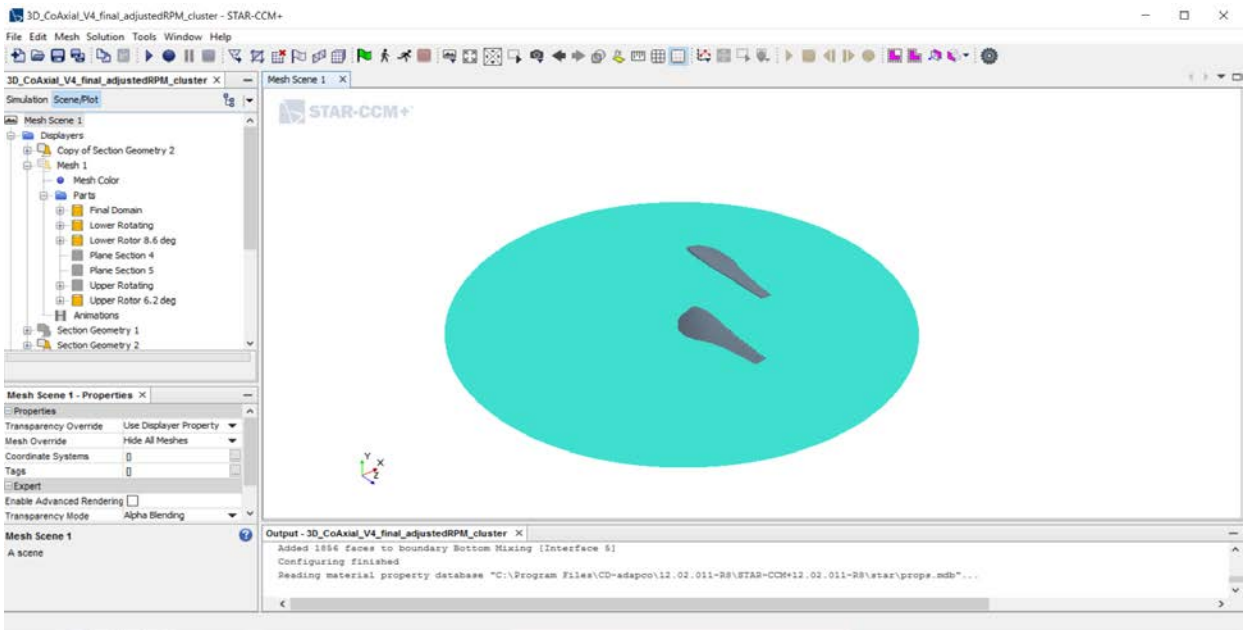

Figure 2. Star-CCM+ Graphical User Interface Ref. 8

The computational resources used in this research include a personal workstation and a computing cluster from the Penn State Aerospace Engineering Department. The workstation, which has sufficient power and memory to both set up the models and visualize the results, has a quad-core processor and 32 Gb of RAM. The computing cluster, COCOA 5, has 1,536 computing cores spread across 48 nodes; this is 32 physical cores per node. The number of nodes for any particular job was chosen to get close to 100,000 cells per core, which was found to provide the most time-efficient balance between computation time per core and communication time between nodes. The required computational time for each model is defined as the number of cores used multiplied by the wall-time. For example, a job that takes two physical hours on 32 cores would have a computational time of 64 hours.

Rotorcraft Analysis Methods

Various methods have been developed to analyze the aerodynamic performance of rotorcraft while balancing the fidelity of the solution with computational cost. On one end of the spectrum are those that model the blades, which have simplifying assumptions that enable fast simulations. This is good for a design in many cases, however, if the airfoil characteristics are unknown and in complex interactions, for example, it may not be well suited to the analysis needed for design. Examples of blade modeled approaches are blade-element-momentum-theory, free-vortex-wake, and actuator-disk methods. On the other end of the spectrum are blade-resolved approaches, which include blade-resolving CFD methods such as RANS, detached eddy simulation, large eddy simulation, and direct numerical simulation. These approaches are referred to as blade resolved because they aim to directly solve a modeled form of the Navier-Stokes

equations around a resolved rotor blade. These high-fidelity models directly account for the blade shape and compute the rotor inflow at a much higher computational cost, which in some cases can have a solution time of several months.

This research proposes a blade-resolved CFD approach using a technology referred to as a mixing plane. The approach retains many of the benefits of blade-resolved methods, but uses assumptions that allow for a large reduction in computational time. The model approach is still able to capture all the relevant aspects of the rotor system, i.e., the loss of lift from the blade-tip vortex, hub effects, and refined wake regions to resolve the rotor-rotor interaction and rotor wake. Figure 3 shows a comparison of the computational requirement versus model fidelity for the various methods.

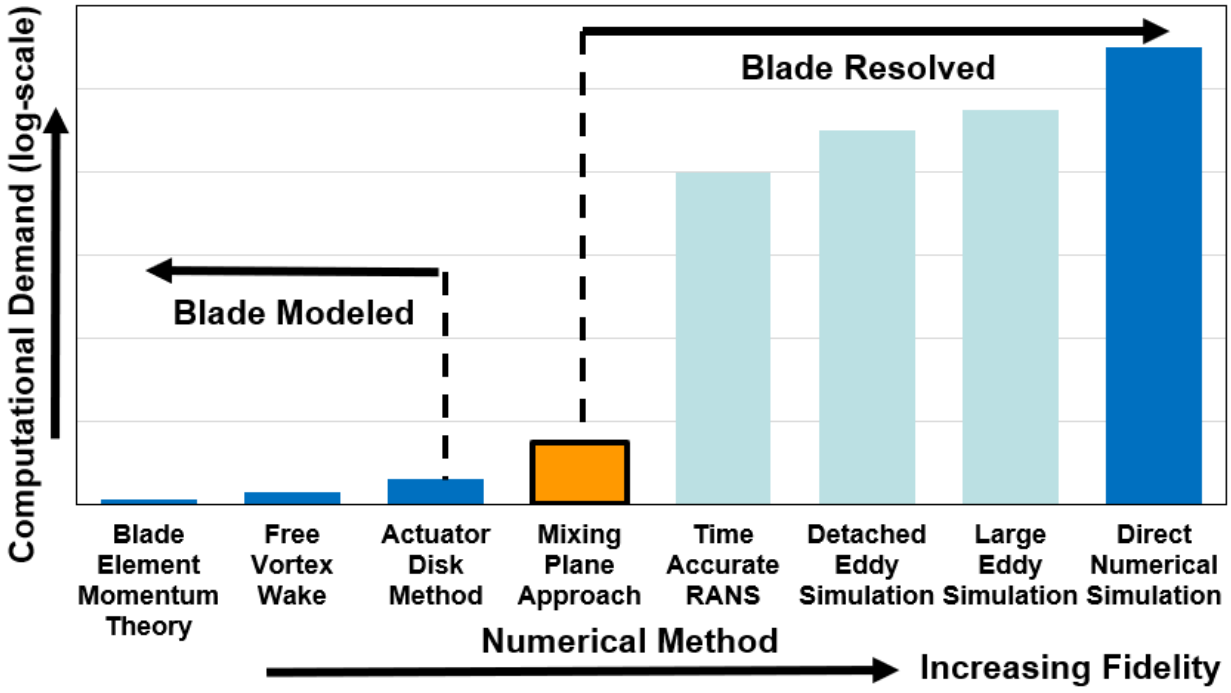

Figure 3. Comparison of Computational Time vs. Model Fidelity for Various Computational Approaches Applied to Co-Axial Rotors. Note: These computational times are based on the authors' guess and not actual data.

Chapter 3

Approach

This research used the STAR-CCM+ CFD software to develop computational models for simulating a co-axial rotor in hover. The development of two final models is presented. The novel approach will be referred to as the Mixing Plane Approach. The Time-Accurate Approach uses conventional rotorcraft CFD methodology. Both approaches are based on the same grid, and the differences only arise in boundary types and solution methods. A step-by-step process was used to develop the models from their initial stage as a two-dimensional (2D) airfoil model to the final co-axial rotor models. The progression of steps taken in the model development process will be presented in the same fashion.

The airfoil model is presented first. In this step, a two-dimensional model was created for the NACA 23012 airfoil. Following grid studies of the Airfoil Model, the Non-Rotating Model was developed. This created the three-dimensional grid that would later be applied to the co-axial rotor. The development of the mixing plane co-axial rotor model is then discussed. Finally, the time-accurate co-axial rotor model is presented. A comparison of results from the two approaches is shown, along with conclusions, future work, and recommendations. Figure 4 shows a road-map of the model progression.

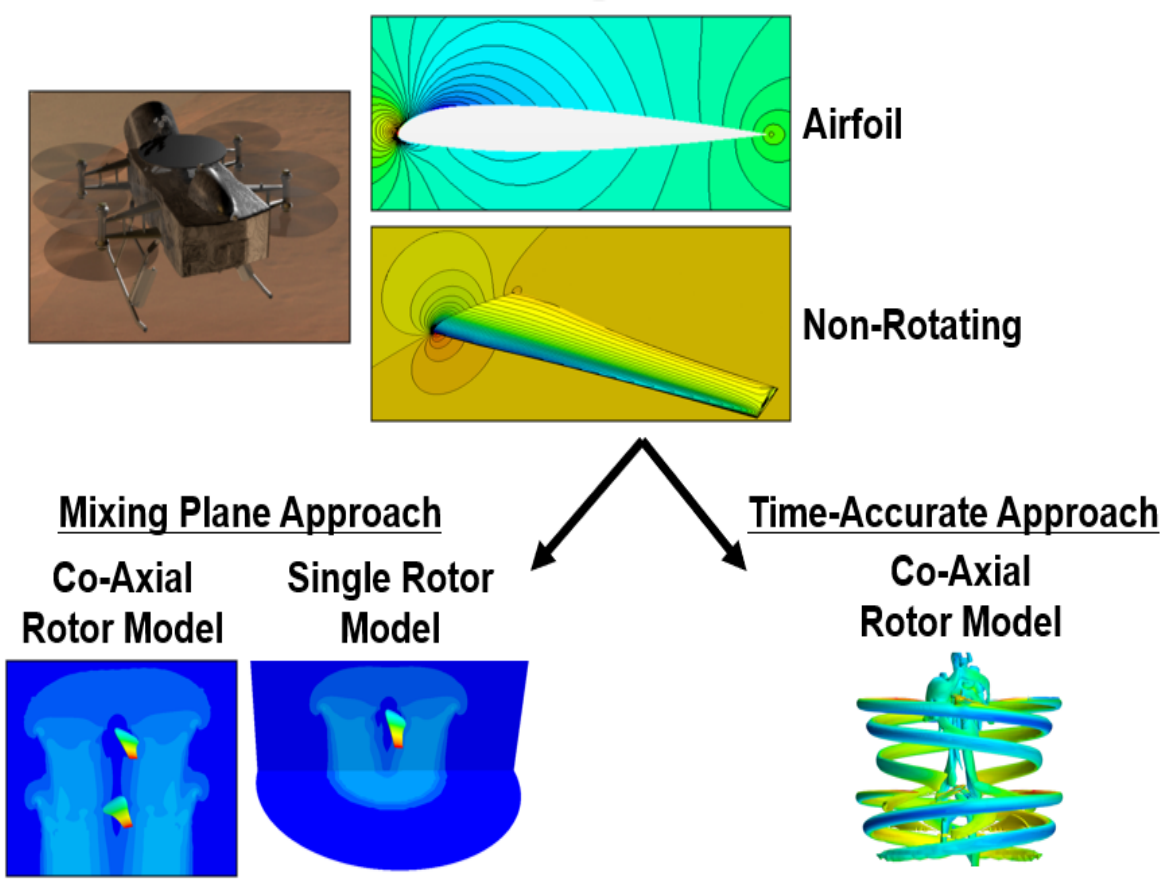

Figure 4. Progression of Model Development

Following the introduction and explanation of the various models, a comparison in performance results and computational parameters will be explored. The comparison will highlight the time-savings of the novel approach while still maintaining a high-fidelity solution. Conclusions will be presented on what the research has made possible, and future direction for the work will also be discussed.

Chapter 4

Development of the Mixing Plane Co-Axial Rotor Model

This section describes the progression of the CFD tool from the initial two-dimensional model to the final co-axial mixing plane rotor model. Each model discussed adds additional features and complexity to the simulation.

Airfoil Model

The first step in creating this analysis tool was to develop the grid around a two-dimensional airfoil. This research used the NACA 23012 airfoil. The model incorporates a C-type grid around the airfoil that is overset with the background domain. The overset boundary allows the angle-of-attack (AOA) to be changed without having to regenerate the grid. The domain boundaries are at twenty-five chord lengths. Figures 5-7 show the near-body grid around the airfoil and the overset boundary, respectively.

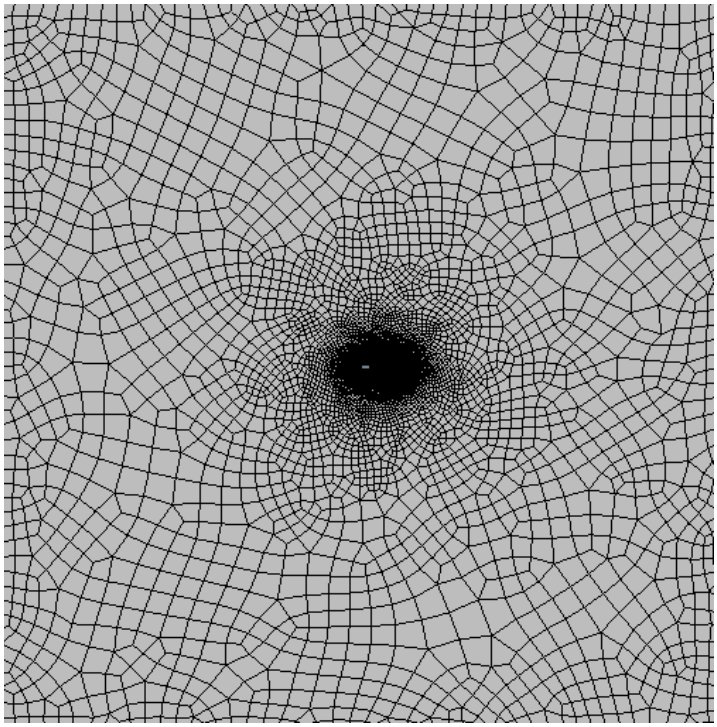

Figure 5. Airfoil Model Background Grid

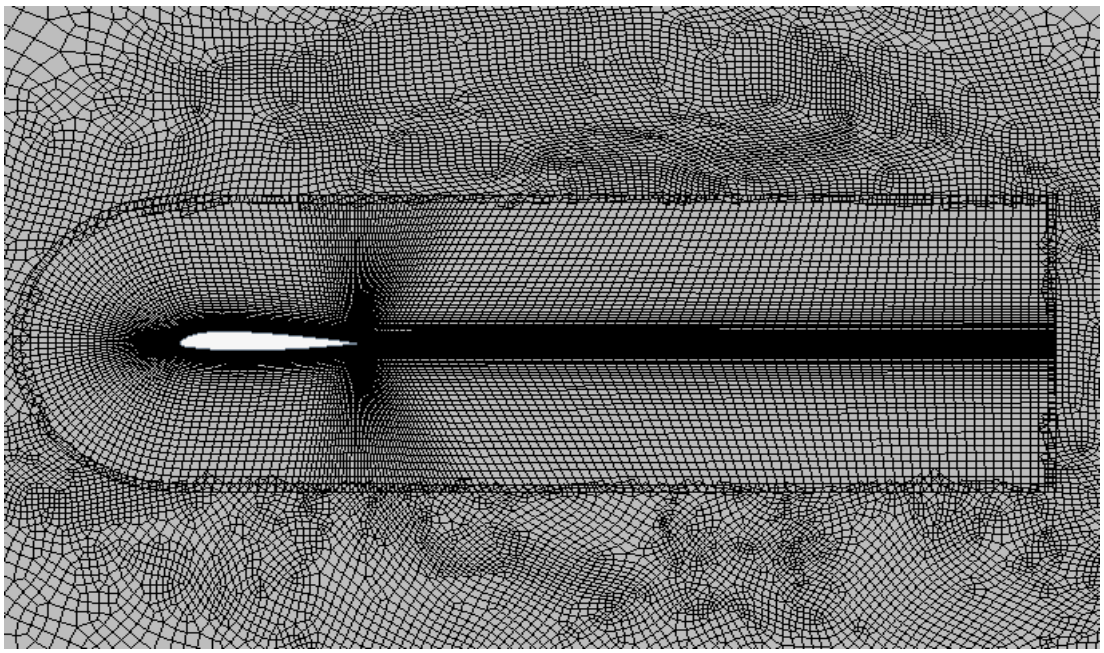

Figure 6. Airfoil Model Overset Grid (NACA 23012)

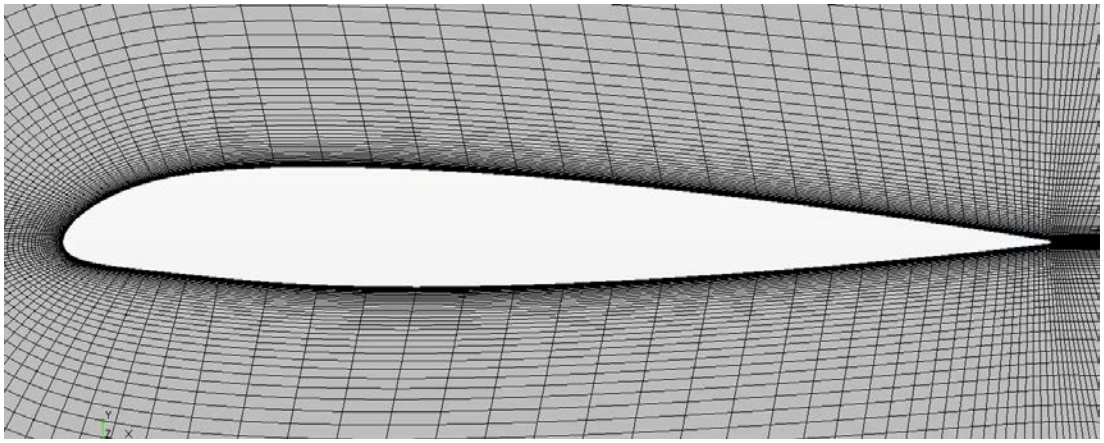

Figure 7. Airfoil Model C-Type Grid (NACA 23012)

A grid refinement study was conducted to optimize the airfoil model. The goal of the optimization was to reduce the overall cell count while maintaining an acceptable fidelity. This is done to keep the final cell count in the three-dimensional models manageable. The model incorporates a quadrilateral unstructured mesh for the background with a volume constraint around where the overset body is located. This forces a 1:1 cell aspect ratio at the overset boundary. The C-type grid was generated using the Star-CCM+ directed mesh tool, which allows for precise control of a structured near-body mesh. The final C-type mesh extends five chord-lengths behind the airfoil and incorporates 131 wrap-around points along the airfoil contour, a trailing-edge chord-wise spacing matching the trailing-edge thickness of 0.23% of the chord-length, a leading-edge chord-wise spacing of 0.20% of the chord-length, and a 15% maximum growth rate on connected cells. A first cell size was selected to give a y-plus equal to 45 based on a chord Reynolds number of 3×10^6. The Star-CCM+ All-y+ wall treatment, a hybrid model that adjusts based on the local y+, is used in the model. A RANS solver with Spalart-Allmaras (SA), Ref. 9, turbulence model was used for the simulation. In addition, a SIMPLE-based segregated solution method is used for

the numerical model (Ref. 10). Figures 8-9 show pressure and velocity contours for the airfoil model at zero AOA, respectively.

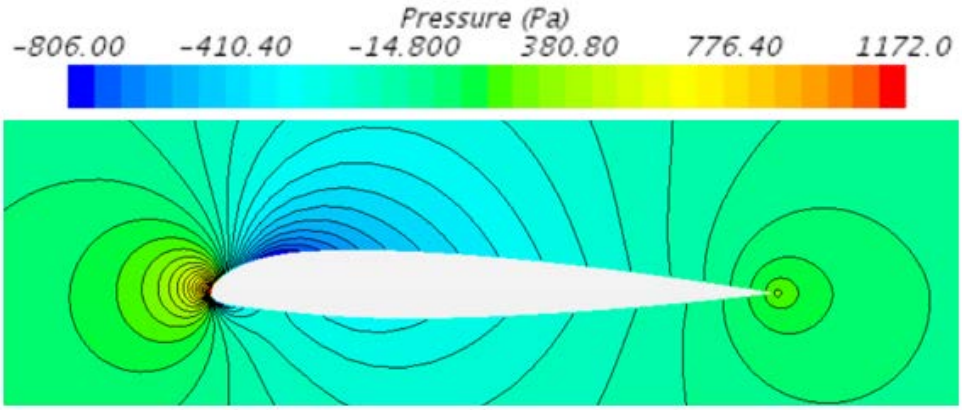

Figure 8. Airfoil Model Pressure Contours (NACA 23012, Re=3x10^6, AOA=0)

A comparison was carried out with data obtained from XFOIL (Ref. 11). The NACA 23012 was analyzed in XFOIL at the same Reynolds number, 3 x 10^6, with forced transition at the leading edge to simulate the fully-turbulent flow in the CFD model. Values of lift coefficient, drag coefficient, and lift-to-drag versus angle of attack were gathered from both XFOIL and the Star-CCM+ model. Plotting the results over top of each other, as seen in Figure 11, shows a strong correlation between the two methods. The lift and drag values matched to within 1% and 8%, respectively. These values also agreed with experimental data in Abbott and Von Doenhoff (Ref. 12). The strong correlation provided sufficient confidence in the model's ability to accurately predict attached boundary layer flows where XFOIL is known to perform well. A model with higher refinement had been closer to the XFOIL values, but the current values were deemed acceptable in order to maintain a reasonable cell count. Figure 12 shows a comparison of the surface pressure coefficient around the airfoil at zero AOA for both XFOIL and Star-CCM+. The

pressure coefficient matches along the entire chord-length, and only a slight deviation is observed at the trailing-edge.

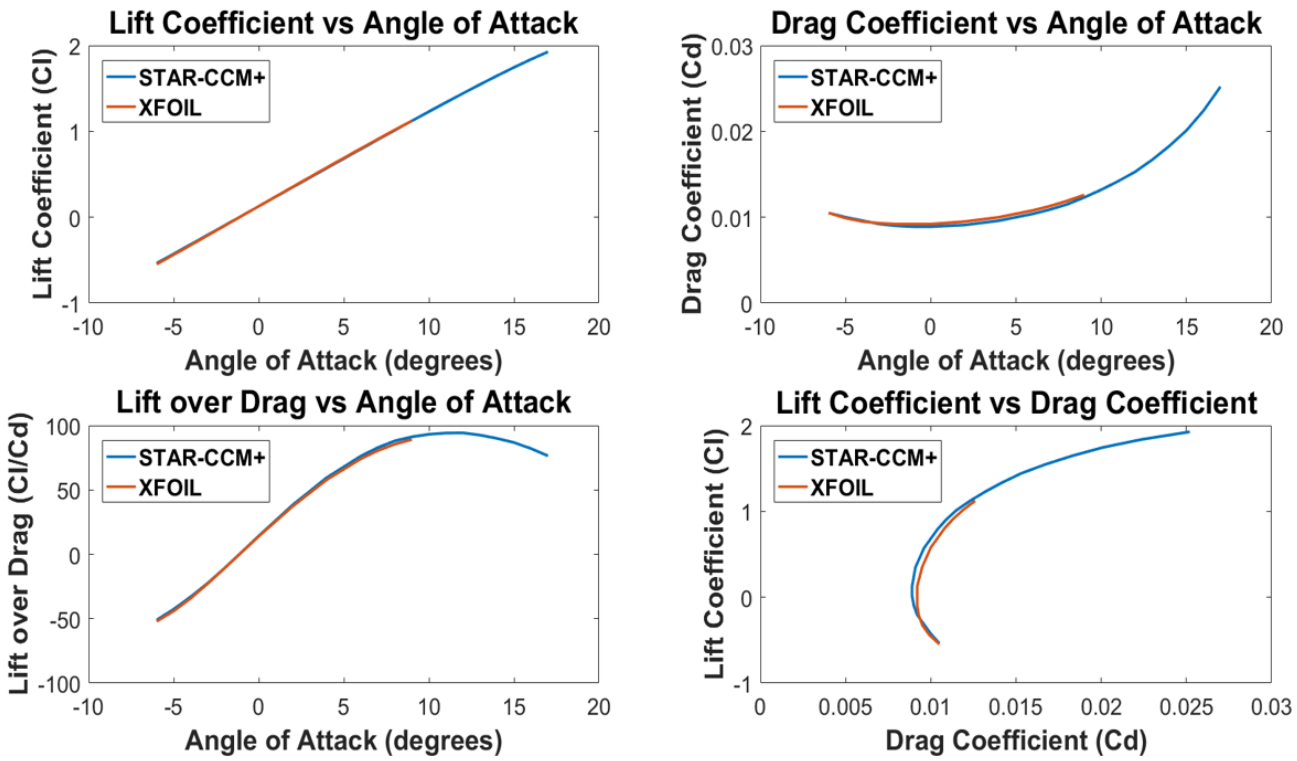

Figure 9. Airfoil Model Comparison with XFOIL Using Performance Coefficients (NACA 23012, Re=3x10^6)

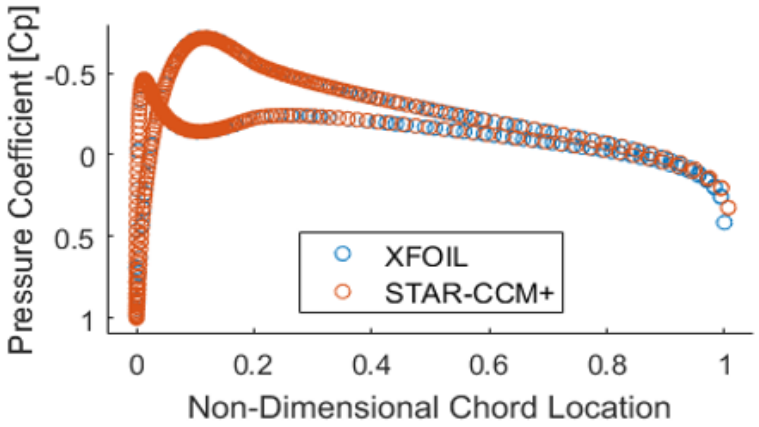

Figure 10. Pressure Distribution Comparison of Airfoil Model and XFOIL (NACA 23012, Re=3x10^6)

Non-Rotating Model

The purpose of the non-rotating model was to implement the optimized two-dimensional airfoil grid into a three-dimensional model. A twist and taper distribution from the Dragonfly rotor design, Ref. 13-14, were used to create a full blade. The grid was generated by extrapolating the C-type mesh along the planform of the blade; this was also done using the directed mesher tool within Star-CCM+.

The model was set up so as to allow for a comparison with PSU-XTurb, Ref. 15, which was used to run a lifting-line theory simulation. This was done imposing a symmetry plane along the maximum chord to simulate a semi-span wing.

A process similar to the extrapolation of the C-type mesh was used for the background and overset regions. A blade-tip refinement methodology was developed to capture the blade tip vortices. The cell size along the span of the blade was adjusted to provide the blade tip cell width close to the first cell thickness. This size was used for the blade tip volume control, and it was then subsequently increased in the off-body region to provide a 1:1 cell volume ratio with the background region at the overset boundary. The simulation uses RANS with SA turbulence closure chosen to accurately model the steady, attached flow. The comparison with PSU-XTurb found the lift to match within 1.5%. This comparison showed that the C-type mesh had been extrapolated correctly to obtain the three-dimensional model. Figures 13-14 show the non-rotating semi-span wing grid and pressure contours, respectively.

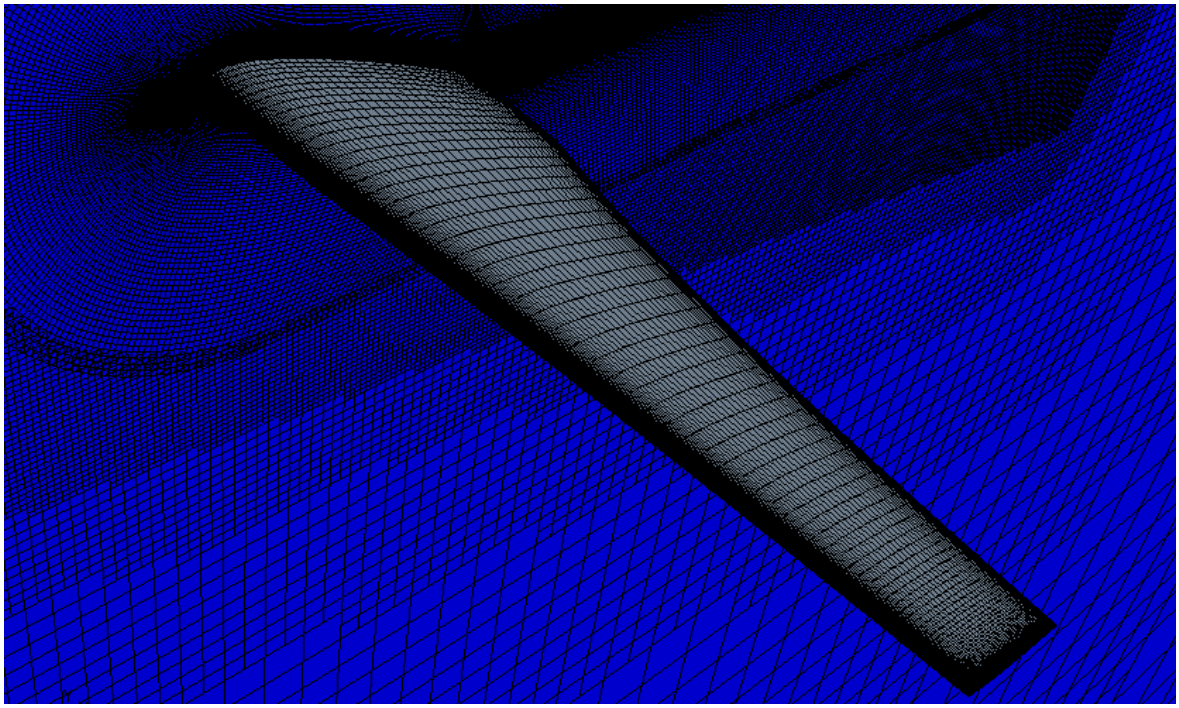

Figure 11. Non-Rotating Blade Model – Grid (Modified Dragonfly Blade Planform)

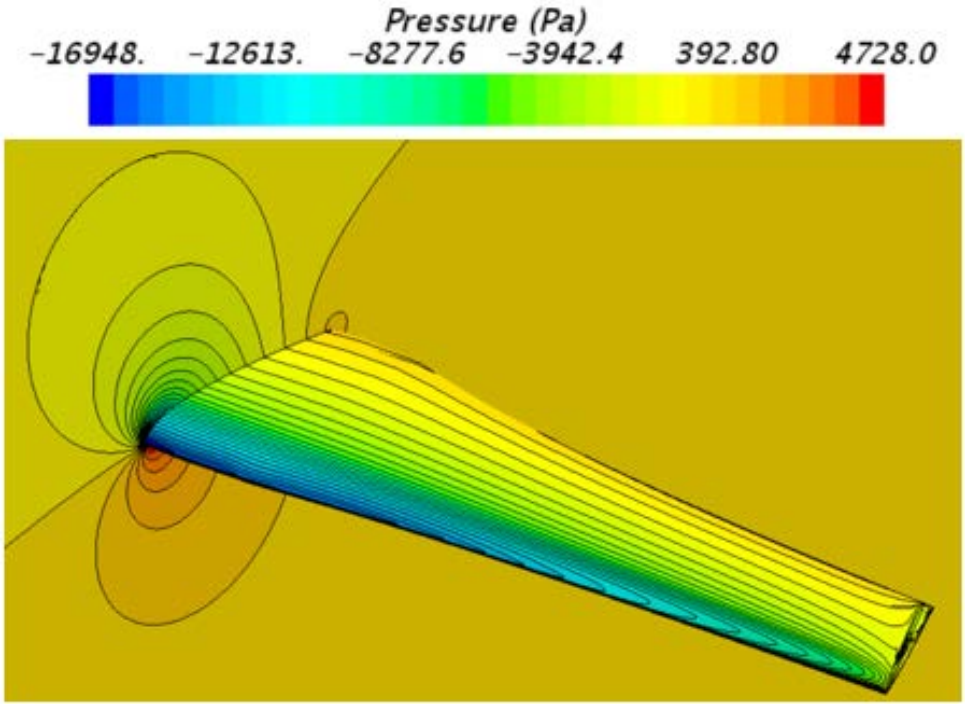

Figure 12. Non-Rotating Blade Model - Pressure Contours (Modified Dragonfly Blade Planform)

Mixing Plane Approach

The next model incorporates the mixing plane boundary type, which is common to turbomachinery applications. The boundary is split into concentric rings or bins, and the flow passing through the boundary is averaged on each individual bin. This provides a circumferentially averaged flow solution at the mixing plane interface.

This proposed CFD approach provides three substantial benefits. The model approach (1) allows for the solution in a rotating reference frame, (2) the usage of periodic boundaries to reduce grid size, and (3) smears the rotor wake reducing the demand for high-resolution rotor wakes. The periodic boundary, which requires only one blade per rotor to be modeled regardless of the number of blades on the rotor, provides a significant reduction in the total cell count. This is because the blades are one of the regions that demand the most computational cells. The ability to use a rotating reference frame is another time saving aspect from this research. This is because the solution becomes a steady solution method, eliminating the need for grid motion and temporal resolution. It will be shown that eliminating the time-accurate aspect of the model is what dominates the computational savings in the present model. Lastly, the present model also alleviates the computational requirements of the rotor wake. For hover, these are normally significant. The present approach eliminates the need to resolve a wake dominated by tip vortices as the mixing plane smears these vortices, and the resulting wake becomes favorable to a coarse rotor-wake mesh.

Figure 15 shows an example of the mixing plane boundary in a turbomachinery application. One blade on both the rotor and the stator are outlined with a periodic boundary, signifying that they are the only blade of each respective stage being modeled. The mixing plane boundary can be seen coming straight down the middle of the diagram.

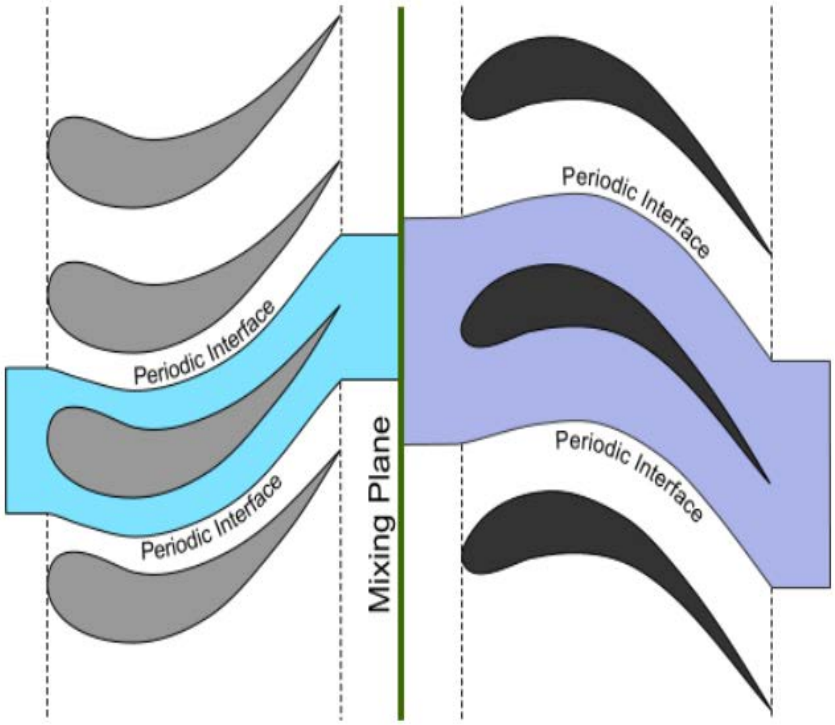

Figure 13. Illustration of Mixing Plane Approach Ref. 8

Mixing Plane Single Rotor Model

This first mixing plane model added in the complexities of a rotating reference frame, the mixing plane boundaries, wake refinement, and a periodic boundary. The modeled aircraft has two-bladed rotors, which means that only one of the two blades is physically included in the grid for the single rotor model as can be seen in Figure 16. The white space in the image represents a void region, half of the cylindrical disk, where there are no grid cells. The periodic boundary maps the flow solution from the modeled blade onto the other half of the region. The bold black lines on the image represent the mixing plane boundary interface. Figure 17 shows another image of the grid including the blade, periodic boundary, and the lower mixing plane boundary. Figure 18

shows velocity contours for the mixing plane single rotor model. The blade tip vortices, contraction of the wake, and hub effects can all be observed.

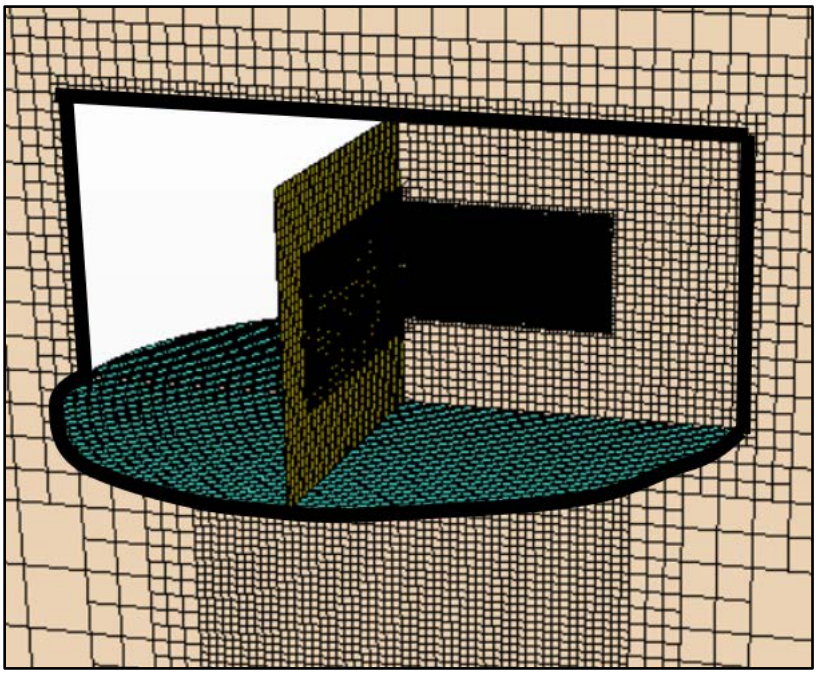

Figure 14. Mixing Plane Single Rotor Model – Grid (Mixing Plane Boundaries Outlined in Black)

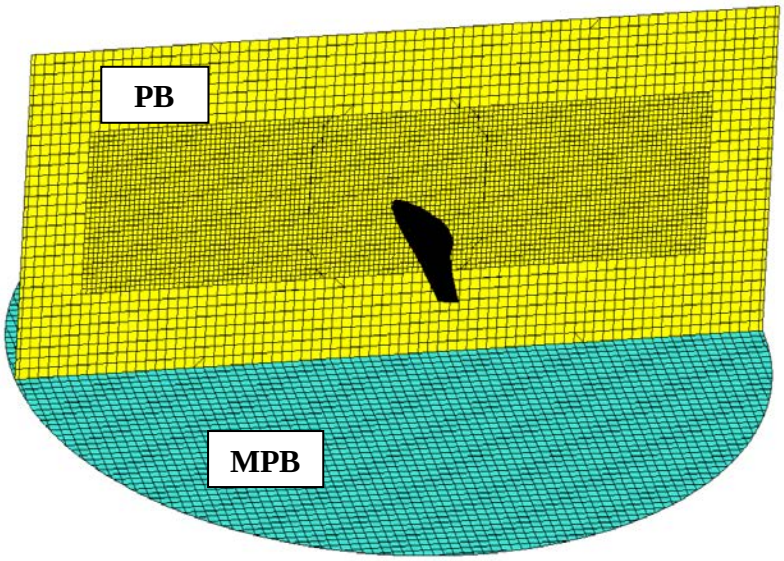

Figure 15. Mixing Plane Single Rotor Model – Periodic Boundary (PB), Mixing Plane Lower Boundary (MPB)

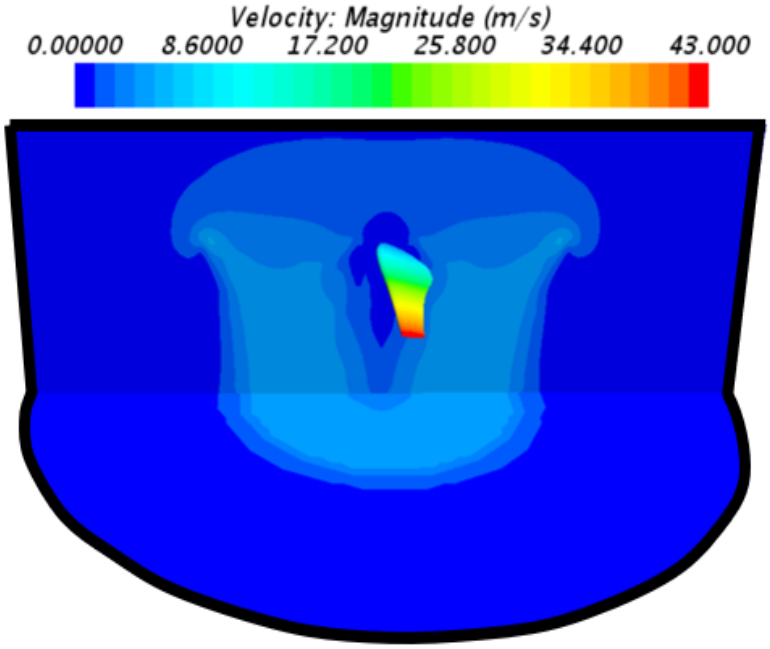

Figure 16. Mixing Plane Single Rotor Model - Velocity Contours on Periodic Boundary and Lower Mixing Plane (Mixing Plane Boundaries Outlined in Black)

Mixing Plane Co-Axial Rotor Model

The mixing plane co-axial rotor model uses the same set up developed for the single rotor model with the second rotor added 0.4 rotor diameters below the first one. The single rotor model had a coarsened grid, since its purpose was only to develop the methodology. This co-axial model re-introduced the refined grid parameters that had been found through the airfoil model and subsequent grid optimization studies. Further grid refinement studies were carried out on this model to determine the required refinement around the blade-tips and in the rotor wake. The model uses counter-rotating reference frames with the mixing plane in-between them. Figure 19 shows the outlined mixing plane boundaries. Figure 20 shows the velocity contours around the blades and in the wake. The lower rotor can be seen operating in the fully-developed contracted wake of

the upper rotor. Figure 21 shows pressure contours at the blade tip. The stagnation point, blade tip vortex, and loss of lift at the tip are all shown.

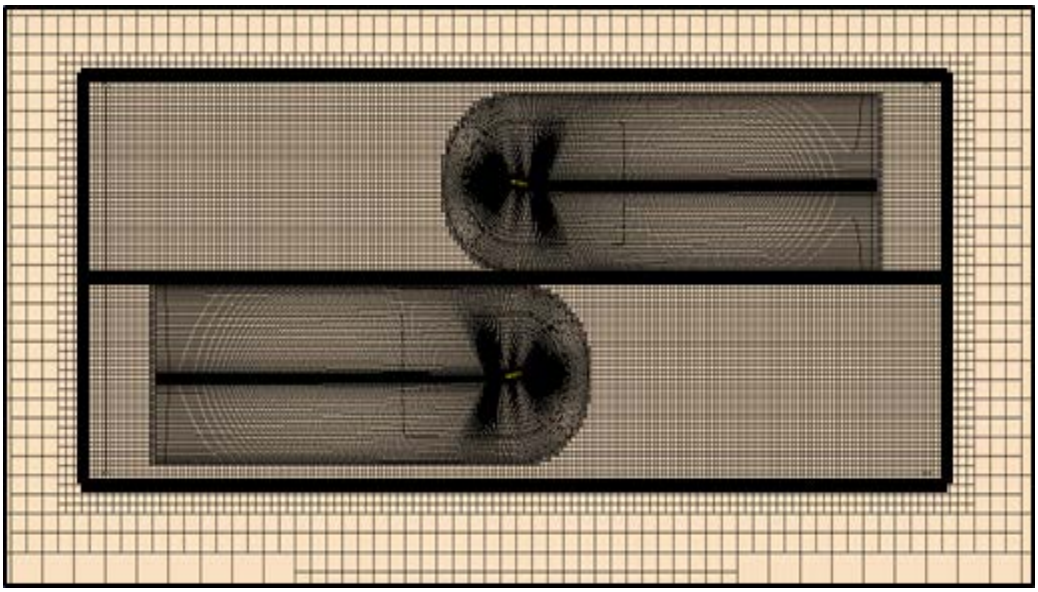

Figure 17. Mixing Plane Co-Axial Rotor Model – Grid
(Mixing Plane Boundaries Outlined in Black)

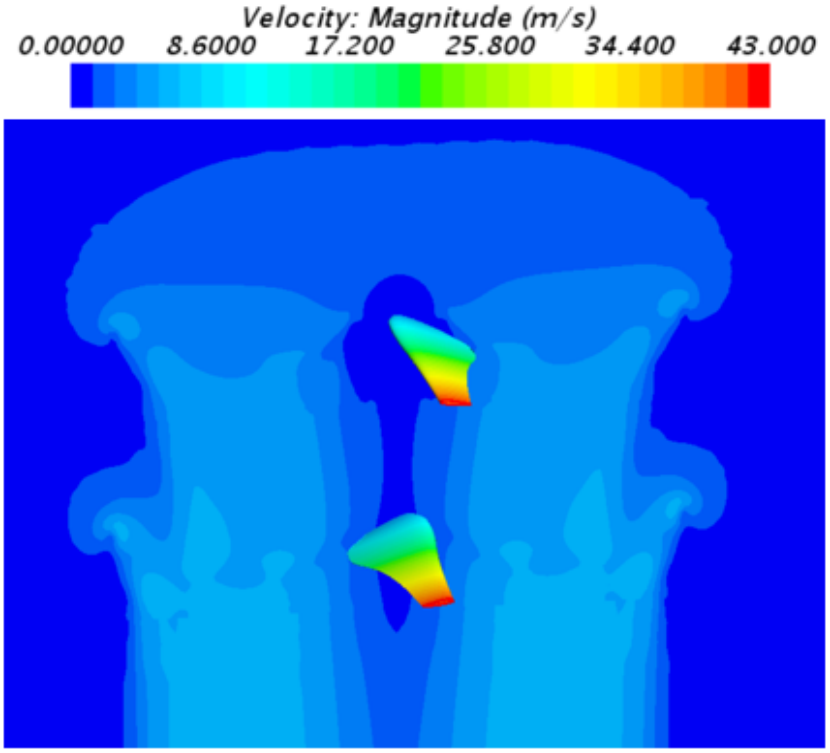

Figure 18. Mixing Plane Co-Axial Rotor Model - Velocity Contours on Periodic Boundary

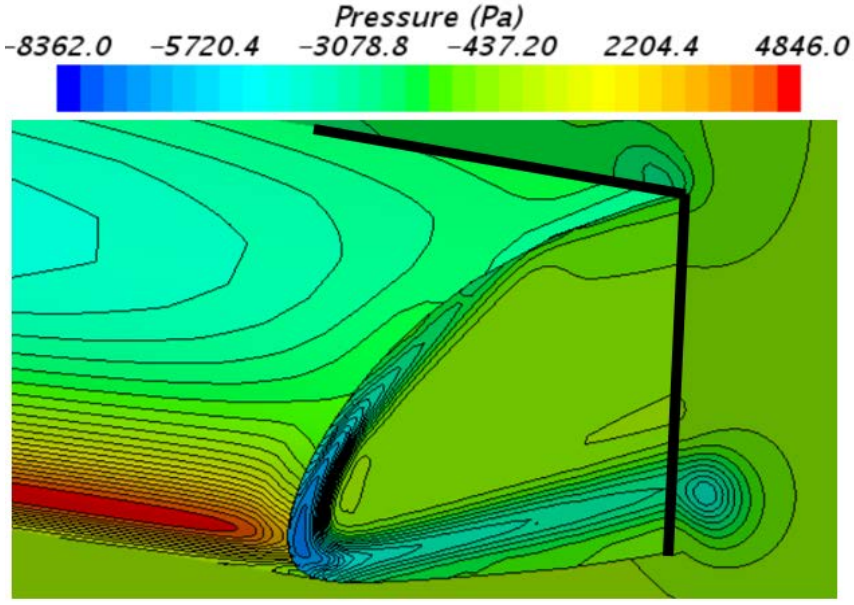

Figure 19. Mixing Plane Co-Axial Rotor Model - Pressure Contours on Blade and Span-wise Cut-plane (Cut-plane Boundary Outlined in Black

Chapter 5

Time-Accurate Co-Axial Rotor Model

In order to make a comparison of the mixing plane approach to conventional best practices, a time-accurate co-axial rotor simulation was run. The near body grids are identical between the two models and the time accurate model includes the two additional blades that were removed from the mixing plane model with the use of periodic boundaries. The total model has 31.9 million cells, roughly twice as many as the mixing plane model. Instead of mixing planes, sliding grid interfaces are used within an unsteady time-accurate RANS solver using an SA turbulence model. The model was run with two different physical time-step sizes of 1.5 degrees and 0.25 degrees that will be referred to as the coarse and refined runs, respectively. Each time step had 20 sub-iterations in order to decrease the residuals by at least two orders-of-magnitude per time step. Figure 22 shows a cross-section of the grid through all four blades and their C-type meshes. Figure 23 shows an isosurface of two rotor revolutions with a Q-criterion of 500 colored by the local velocity.

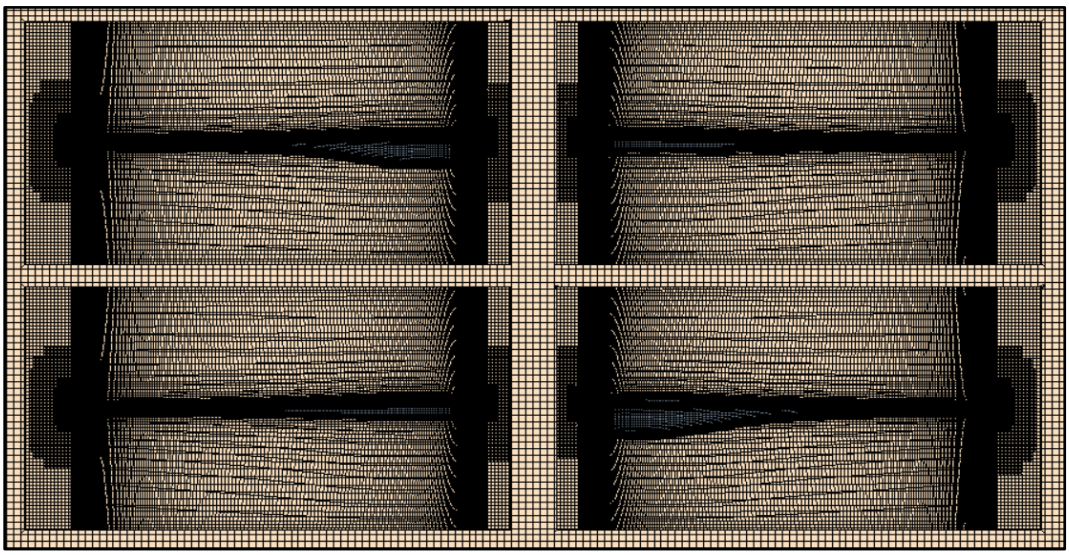

Figure 20. Time-Accurate Co-Axial Rotor Model – Grid
(Four Blades with C-type Grids Shown)

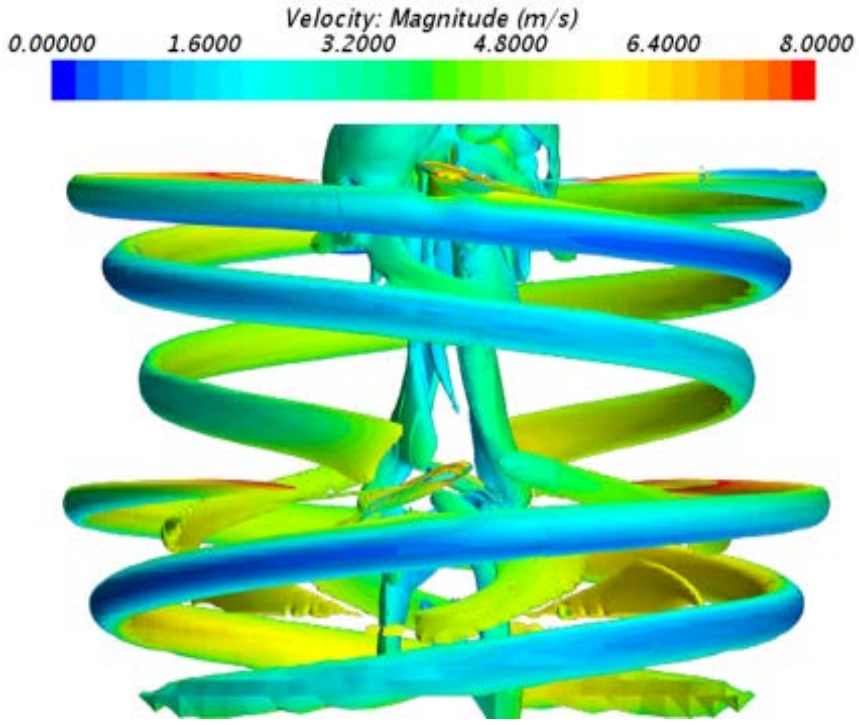

Figure 21. Time-Accurate Co-Axial Isosurface – Q-Criterion = 500 [1/s^2]
Flow After 2 Revolutions Shown

Chapter 6

Results

Rotor performance metrics such as thrust, torque, and figure of merit have been gathered from both the novel mixing plane and time-accurate approaches. Information related to the computational models such as cell count and computational time have also been tracked. Figure 24 shows the total co-axial rotor thrust, individual rotor torques, total cell count, and computational time for the coarse time-accurate model (1.5 degree time-steps) versus the mixing plane model; Figure 25 shows the same information for the refined time-accurate model (0.25 degree time-steps) versus the mixing plane model. The cell count is plotted in millions and the computational time, which is defined as the number of physical hours the simulation was run multiplied by the number of cores, is plotted in thousands of hours. The percentages shown in the figures and in the tables are percent differences between the two approaches, which is comparing the accuracy of the novel mixing plane approach to the widely accepted time-accurate solution method. Tables 2-3 show the same information as Figures 24-25, respectively, along with additional parameters.

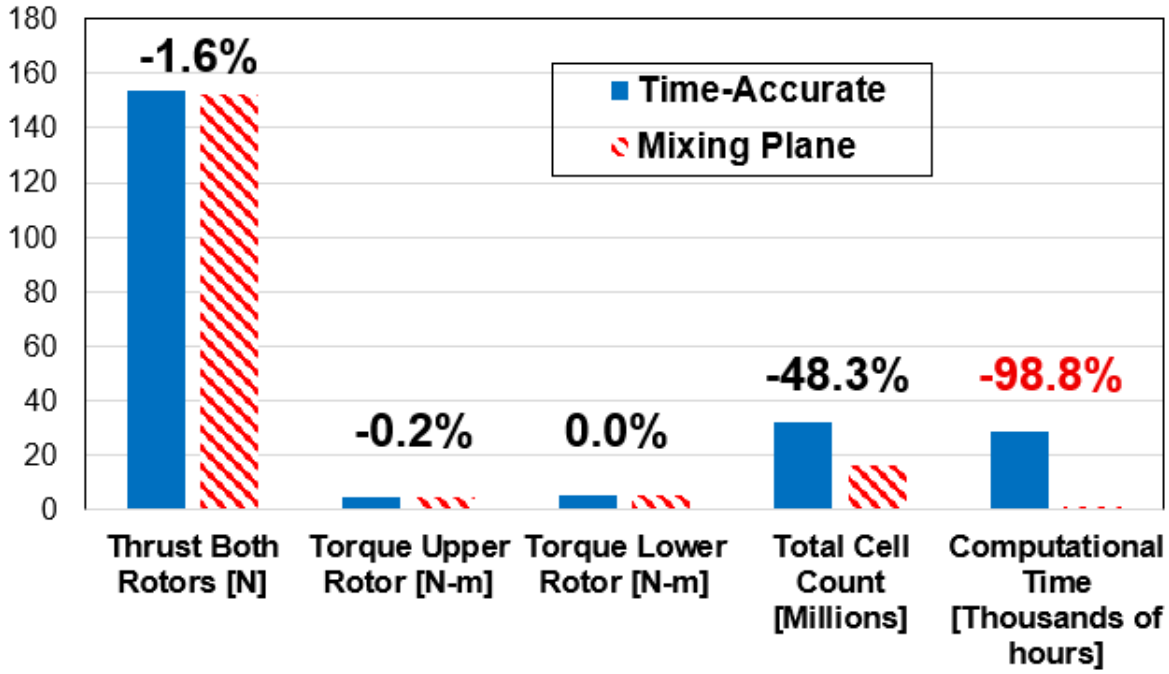

Figure 22. Results for Coarse Time-Accurate Model (1.5 Degree Time-steps) vs. Mixing Plane Model

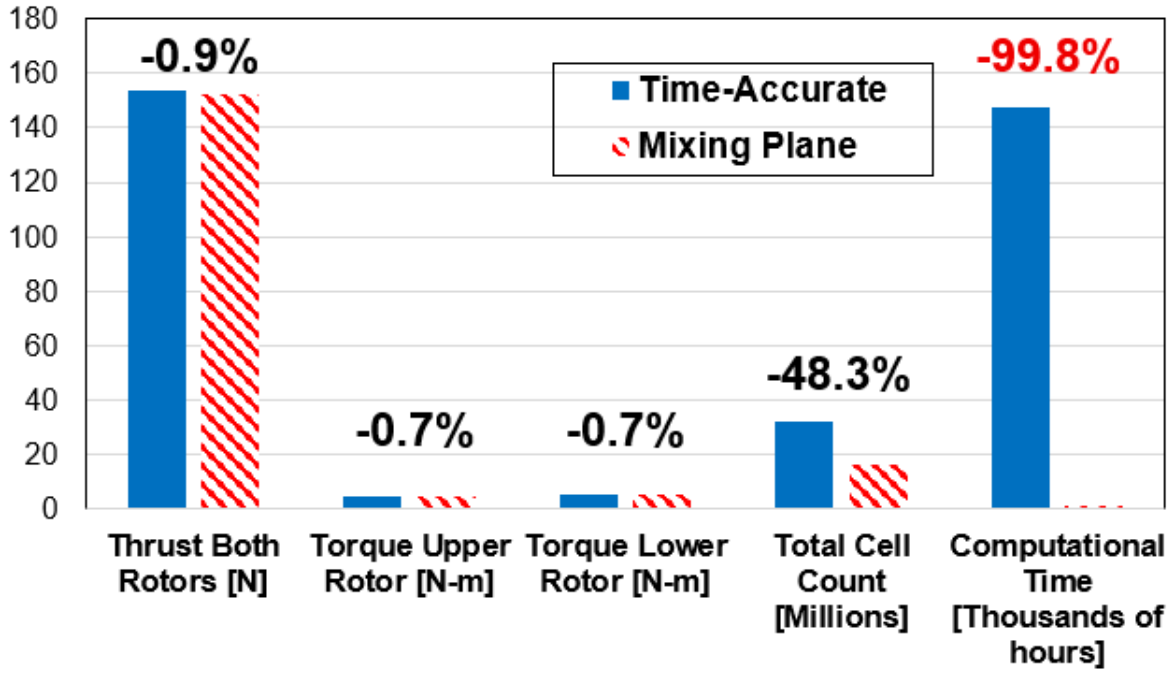

Figure 23. Results for Refined Time-Accurate Model (0.25 Degree Time-steps) vs. Mixing Plane Model

Table 2. Results for Coarse Time-Accurate Model (1.5 Degree Time-steps) vs. Mixing Plane Model

Model Parameter	Time-Accurate Model	Mixing Plane Model	Percent Difference
Thrust Both Rotors	154.7 N	152.2 N	-1.6 %
Thrust Upper Rotor	79.9 N	78.2 N	-2.1 %
Thrust Lower Rotor	74.9 N	74.0 N	-1.2 %
Figure of Merit	0.773	0.755	-2.3 %
Torque Upper Rotor	4.43 N-m	4.42 N-m	-0.2 %
Torque Lower Rotor	5.52 N-m	5.52 N-m	0.0 %
Physical Blades	4	2	-50 %
Cell Count	31.9 M	16.5 M	-48.3 %
Computational Time	28,480 hr	343 hr	-98.8 %

Table 3. Results for Refined Time-Accurate Model (0.25 Degree Time-steps) vs. Mixing Plane Model

Model Parameter	Time-Accurate Model	Mixing Plane Model	Percent Difference
Thrust Both Rotors	153.6 N	152.2 N	-0.9 %
Thrust Upper Rotor	79.6 N	78.2 N	-1.8 %
Thrust Lower Rotor	74.0 N	74.0 N	0.0 %
Figure of Merit	0.767	0.755	-1.6 %
Torque Upper Rotor	4.45 N-m	4.42 N-m	-0.7 %
Torque Lower Rotor	5.48 N-m	5.52 N-m	0.7 %
Physical Blades	4	2	-50 %
Cell Count	31.9 M	16.5 M	-48.3 %
Computational Time	147,587 hr	343 hr	-99.8 %

Chapter 7

Conclusions and Future Work

Throughout this work a three-dimensional computational fluid dynamics model for the analysis and optimization of multicopter aircraft has been developed. The model incorporates a novel approach using mixing plane boundaries that allow for the use of periodic boundaries, rotating reference frames, and a steady RANS solver. Theoretical calculations were used in conjunction with grid-refinement studies throughout the development of the model to optimize the grid parameters. This resulted in a high-fidelity grid capable of capturing the relevant aspects of the rotor system, i.e., the loss of lift from the blade-tip vortex, hub effects, rotor-rotor interactions, and the rotor wake.

The same grid parameters were used to create a conventional time-accurate model. Results were presented comparing the rotor performance between the conventional time-accurate model and the novel mixing plane approach. The time-accurate model was run once with coarse 1.5 degree time-steps and once with refined 0.25 degree time-steps. The results comparing the refined time-accurate model with the mixing plane model show the largest deviation as the upper rotor thrust at 1.8%. The computational time to arrive at this result was reduced by 99.8%. This is a 430 times reduction in computational time, or more than two orders-of-magnitude. In the present research, this meant getting nearly an identical answer in two hours instead of more than two and a half weeks.

Another benefit observed in the mixing plane model is the largely reduced overall cell count, which was a 48.3% reduction. This was realized through the use of periodic boundaries, which the mixing plane approach allows for even in a co-axial simulation. Mixing plane simulations were thus run on half the number of cores as compared to the time-accurate approach, which likely also contributes to the time savings since there is less communication required between nodes on the cluster.

The research accomplished its goal to create an analysis tool for optimization of the Dragonfly aircraft, and the insights gained can potentially increase design capabilities for future multicopter aeronautical concepts. The performance results obtained for Dragonfly will be used in an iterative design process to develop a mission ready vehicle. Theoretical design methods from Leishman, Ref. 16-17, are now being used to further guide the co-axial rotor analysis and optimization.

Research has been started on implementing the mixing plane approach in forward-flight cases. A similar process is being used by comparing the mixing plane forward-flight model to a conventional time-accurate model. One issue in forward flight is that some of the mixing-plane treatments breakdown, hence, the model will likely only be successful for low advance ratios. Nevertheless, such a tool still may provide value as a design tool and advanced mixing-plane approaches may be implemented to advance the method to forward flight. Aircraft geometry is also being added to the model to allow for full aircraft performance analyses. An already flying Dragonfly scale-model at Penn State University is planned to gather experimental data for future model validation.

Appendix A

Airfoil Model Set-Up

Introduction

This section will go through the setup of the 2D airfoil model from geometry creation to model configuration. The software tools used to create this model include the SolidWorks computer aided design (CAD) program and the STAR-CCM+ CFD program. XFOIL and MATLAB were used to investigate the accuracy of the CFD model, as well as carry out the grid refinement study.

Geometry Creation

The geometry for the 2D model was created using the CAD program SolidWorks. Any CAD program that can save the files with an X_T filetype can be used. The STAR-CCM+ software also includes its own CAD modeling package, which would likely also be able to create the required geometry. For convenience down the road with the 3D models, the process was developed to import the SolidWorks created geometry.

The 2D airfoil model has three different part-bodies: the background domain, the C-type grid, and the overlap area. The C-type grid is a structured on-body grid that allows for detailed control of cell settings at the airfoil. The C-type grid is overset with the background domain, which has the boundary conditions and brings the flow in from the far-field. The overlap area is used as a volumetric refinement to ensure that all cells in the overlap area have a 1:1 aspect ratio with the

C-type mesh cells at the overset boundary. This means that they are the same size, which is recommended for the overset interface.

The following procedure details the creation of the geometry for the C-type grid portion. In SolidWorks, first insert the airfoil coordinates using the “Insert curve through x-y-z coordinates” function. Using a Microsoft Excel spreadsheet, insert the airfoil’s X-Y coordinates into the first two columns. The x-coordinates should place the quarter chord at zero. A chord of one meter was used for simplicity in calculating airfoil performance. The chord can be changed by scaling the x and y coordinates by the desired chord length about the quarter chord. For example, to make a chord of 0.18 meters, multiply the x and y coordinates, with a chord length of one, by 0.18. Then enter the value “0” for each row in the third column. Leave the trailing-edge dis-connected for now. These three columns are then copied and pasted into the SolidWorks “insert curve through x-y-z coordinates” function. Once the airfoil is inserted as a curve, change the curve to a sketch by using the “convert entities” function in the sketch toolbar. Add the trailing-edge by editing the sketch, and using a line to connect the trailing-edge. Now create an outline around the airfoil that will be your C-type grid boundary. The boundary is created in two steps. First outline the top, bottom, and right side of a rectangle starting one chord length directly above the airfoil leading-edge that extends five chord lengths behind the leading-edge. These metrics were shown to work well, but could be adjusted depending on the model requirements. A co-axial rotor, for example, may use a smaller vertical spacing to the C-type boundary. Close the front of the C-type body boundary using a semi-circle. The semi-circle should originate directly above the leading-edge, and terminate directly below it. The final step involves extruding the sketch. The length of the extrusion is arbitrary, 0.1 meters was used. If the airfoil was not cut out of the body, use an extruded cut with the airfoil portion of the sketch to remove it.

The background domain for the model is a square box with boundaries set twenty-five chord lengths away from the origin in each direction. Create a sketch with these, or the desired parameters, and extrude it the same distance as the C-type body (0.1 meters in this research).

The overlap body was created in STAR-CCM+, however, it could be created with SolidWorks. It consists of a 2D sketch of an ellipsoid, with center at (2.5, 0) meters, a horizontal major radius of 4 meters, and a vertical minor radius of 2.25 meters. These values were selected such that rotating the C-type body about the origin, which is the quarter chord of the airfoil, always left the C-type boundary within the ellipsoid. Trial and error can be used to find these dimensions, or trigonometry to get it on the first try. Extrude the ellipsoid the same amount as the other two part-bodies.

All of the required geometry is now created. Save the three files with the X_T filetype extension, and be sure to increase the tessellation resolution for best results. The next step involves inserting the geometry, creating the grid, and setting the model parameters.

Model Setup

Open a new model in STAR-CCM+. Insert the three X_T files one at a time by selecting "File → Import → Import Surface Mesh." Check the box "Show Detailed Tessellation Parameters." It was found that reducing the original settings by two orders of magnitude worked well. This gave a "Curve Chord Tolerance" equal to 0.0003, a "Curve Chord Angle" equal to 0.08, a "Surface Plane Tolerance" equal to 0.0003, and a "Surface Plane Angle" equal to 0.08.

Open the surfaces folder for both the background body and the C-type body. Right-click one of the surfaces and select "Split by Patch." For the background body, name the inlet, outlet,

upper wall, lower wall, 2D grid surface, and top-z face. For the C-type body name the inlet, outlet, upper wall, lower wall, 2D grid surface, top-z face, airfoil, and airfoil trailing-edge. Right-click each of the two part-bodies and select “Assign Parts to Regions.” Select the first option in the drop-down box for the first two drop-down menus. “Create a Region for Each Part” and “Create a Boundary for Each Part Surface.” Once the regions have been created, right-click the operations folder under geometry and select “New → Mesh → Badge for 2D Meshing.” Select the background and C-type body and execute the command. The bodies are now ready for generating the grid.

Using the operations folder, create an “Automated Mesh (2D)” for the background, and a “Directed Mesh” for the C-type body. For the C-type mesh, set the “top-z face” as the source surface and the “2D grid surface” as the target surface. Right-click the directed mesh and select edit, then create a patch mesh. Here is the video that details the process: https://thesteveportal.plm.automation.siemens.com/articles/en_US/Video/How-to-create-a-structured-2D-mesh-inside-STAR-CCM

Set the desired mesh parameters for the background body, and add a volumetric refinement using the overlap body under custom controls. Set the cell size within the refinement to the boundary size of the C-type mesh.

Appendix B

Non-Rotating Blade Model Set-Up

The 3D model was created by extrapolating the validated 2D C-type mesh. Twist and taper distributions were used in the first step of geometry creation to create a full blade in SolidWorks. The blade was "cut" at the maximum chord and the root was then discarded. Starting the blade at the maximum chord thickness and utilizing a symmetry plane there allows for the blade to simulate a semi-span wing. This was key in order to compare the CFD result with PSU-XTurb, which later gave additional confidence in the mesh. A similar process was used to generate this mesh as was used for the 2D airfoil mesh. This involved creating the body encasing the blade, and a background body.

In STAR-CCM+, the directed mesher was used just as in the 2D airfoil model to create the structured on-body mesh. This allows for high control on the prism layers and wake refinement behind the blade. Similar best practices as used in the 2D model were used when transitioning between the blade-body boundary and the background-body. A tip-refinement body was created that had the same shape as the blade-body so as to butt up against the end of the blade-body. This allowed for volumetric refinements to be used on and around the blade-tip. A mesh convergence study was conducted to determine the amount of tip-refinement needed to properly capture the effects of the blade-tip-vortices. This is done by increasing the refinement through altering one parameter at a time and noting the deltas in the simulation's calculations such as lift and drag on the blade (semi-span wing in this case). When the deltas become small compared to the high increases in cell count required to achieve them, this can be considered your "converged CFD solution". This converged value may still be different than the true physical value, but it is what can be obtained with present day modeling and computing capabilities.

Appendix C

Co-Axial Rotor Model Setup

This section encompasses the creation of the model for both the mixing-plane and time-accurate models. The geometry for both models is identical, with the only exception being that the mixing-plane has two blades, one on each rotor, while the time-accurate method has all four blades.

The geometry creation follows the same pattern as the previous non-rotating model. The first blade is created in the same manner, being set within a "blade-body." Two of these must be created, the second a mirror-image of the first, in order to model both rotors. This is easily done in SolidWorks using a mirror feature. Additionally, in this step, a rotor disk is created that will house the blade-bodies. The rotor disk is a cylindrical body that extends slightly above and below the blade-body, which allows for changes in the rotor collective values. The blade-body was subtracted from the rotors, so that an internal interface could be used as opposed to an overset interface. The internal interface is a more conservative method. The two rotor disks are stacked one on top of the other, with the blades set inside them (two blade-bodies on the mixing-plane model and four blade-bodies on the time-accurate model). The two blade-bodies from the mixing-plane model can be "mirrored" within STAR-CCM+ to create the full co-axial rotor system without having to redo the entire importing process. The rotor disk setup is within the larger background domain.

After importing the geometry, the boundaries can be set. For the mixing-plane model, mixing planes are set as the boundary type between the rotor disks and the background, and also on the interface between the two rotor disks. Overall there are five mixing planes; one on the top, one on the upper rotor disk's side, one in-between the two rotor disks, one on the lower rotor disk's side, and one on the bottom of the lower rotor disk. For the time-accurate model, all of these boundaries are internal-interfaces.

Mesh parameters from the non-rotating model were used as a base point in this model. A root-refinement body was also added to the blade-bodies, which was in addition to the tip-refinement body from the non-rotating model. A mesh convergence study was then carried out to ensure an appropriately converged CFD solution had been reached in the now rotating simulation.

For simulating motion on the mixing-plane model, a reference frame is used within each rotor disk. This allows the geometry to stay stationary, and thus the solution method is run as steady, which is where immense computational time savings are realized. As for the time-accurate method, rigid-body motion is specified for each rotor disk and blade-body, such that the upper components and lower components all rotate in unison. The time-step was set to allow for 1.5 degree, and later 0.25 degree, marches in the rotor azimuth with each time-step. Each time-step also had a number of sub-iterations that was found to drop the residuals by at least two-orders-of-magnitude.

BIBLIOGRAPHY

1. Young, L. A., “Conceptual Design Aspects of Three General Sub-Classes of Multi-Rotor Configurations: Distributed, Modular, and Heterogeneous,” The 6th AHS Specialists Meeting on Unmanned Rotorcraft Systems, Scottsdale, Arizona, Jan. 2015.
2. Russell, C., Jung, J., Willink, G., and Glasner, B., “Wind Tunnel and Hover Performance Test Results for Multicopter UAS Vehicles,” The 72nd AHS Annual Forum, West Palm Beach, Florida, May 2016.
3. Yoon, S., Lee, H. C., Pulliam, T. H., “Computational Analysis of Multi-Rotor Flows,” AIAA Paper 2016-0812, The 54th AIAA Aerospace Sciences Meeting, San Diego, California, Jan 4-8, 2016.
4. Yoon, S., Lee, H., Pulliam, T., “Computational Study of Flow Interactions in Coaxial Rotors,” American Helicopter Society Technical Meeting on Aeromechanics Design for Vertical Lift Proceedings, San Francisco, CA, January 2016.
5. Yoon, S., Chan, W. M., and Pulliam, T. H., “Computations of Torque-Balanced Coaxial Rotor Flows,” AIAA Paper 2017-0052, The 55th AIAA Aerospace Sciences Meeting, Gaylord, Texas, Jan. 2017.
6. Yoon, S., Diaz, P., Boyd, D., Chan, W., Theodore, C., “Computational Aerodynamic Modeling of Small Quadcopter Vehicles,” American Helicopter Society 73rd Annual Forum Proceedings, Fort Worth, TX, May 2017.
7. Dragonfly, Applied Physics Laboratory, John Hopkins University, 2018. dragonfly.jhuapl.edu
8. Siemens, “User Guide: Star-CCM+ Version 12.06,” (2017).

9. Spalart, P., Allmaras, S., “A one-equation turbulence model for aerodynamic flows,” Paper AIAA 30th Aerospace Sciences Meeting and Exhibit, Reno, NV, Jan 6, 1992.
10. Mathur, S. R., Murthy, J. Y., “A Pressure-based Method for Unstructured Meshes,” Numerical Heat Transfer, Vol. 31, (2), 1997, pp 195-215. Doi: 10.1080/10407799708915105
11. Drela, M., “XFOIL: An Analysis and Design System for Low Reynolds Number Airfoils,” Low Reynolds Number Aerodynamics, Springer, Berlin, Heidelberg, 1989, pp 1-12.
12. Abbott, I. H., and Von Doenhoff, A. E., Theory of Wing Sections: Including a Summary of Airfoil Data, National Advisory Committee for Aeronautics, Langley, VA, 1945, pp. 146.
13. Langelaan, J., Schmitz, S., Palacios, J., Lorenz, R., “Energetics of Rotary-wing Exploration of Titan,” 2017 IEEE Aerospace Conference Proceedings, Big Sky, MT, 4-11, March 2017. Doi: 10.1109/AERO.2017.7943650
14. Lorenz, R. D., Turtle, E. P., Barnes, J. W., Trainer, M. G., Adams, D. S., Hibbard, K. E., Sheldon, H. C., Zacny, K., Peplowski, P. N., Lawrence, D. J., Ravine, M. A., McGee, T. G., Sotzen, K. S., MacKenzie, S. M., Langelaan, J. W., Schmitz, S., Wolfarth, L. S., Bedini, P. D., “Dragonfly: A Rotorcraft Lander Concept for Scientific Exploration at Titan,” John Hopkins APL Technical Digest, 2017.
15. XTurb-PSU A Wind Turbine Design and Analysis Tool, XTurb-PSU, Schmitz, S., 2012.
16. Leishman, J. G., Principles of Helicopter Aerodynamics, Cambridge University Press, New York, NY, 2000, Chapter 10.
17. Leishman, J. G., Ananthan, S., “Aerodynamic Optimization of a Coaxial Proprotor,” American Helicopter Society 62nd Annual Forum Proceedings, Phoenix, AZ, May 9-11, 2006.

Jason K. Cornelius

NSF Graduate Research Fellow
Department of Aerospace Engineering
The Pennsylvania State University, University Park, PA 16802
Phone: 570-332-2300 Email: joc5693@psu.edu

Education

Master of Science, Aerospace Engineering — Planned August 2019
The Pennsylvania State University,

Bachelor's Degree, Aerospace Engineering, Minor in Russian — August 2018
Schreyer Honors College, The Pennsylvania State University,

Professional Experience

July-Aug. 2018 — **Rotorcraft Aeromechanics Intern**
Aeromechanics Branch, NASA Ames Research Center

Aug. 2016-Present — **NSF Graduate Research Fellow**
Department of Aerospace Engineering,
The Pennsylvania State University

June-Aug. 2017 — **Rotorcraft Aeromechanics Intern**
Aeromechanics Branch, NASA Ames Research Center

June-Aug. 2016 — **CFD Intern**
Flight Technology Research and Development Group, Bell Helicopter

Jan.-April 2016 — **Rotorcraft Aeromechanics Intern**
Aeromechanics Branch, NASA Ames Research Center

May-Aug. 2015 — **Rotorcraft Analysis Intern**
Mechanical Analysis Group, Bell Helicopter

Jan. 2015 — **Bell Helicopter Boot Camper**
Student Program Participant, Bell Helicopter

June-Aug. 2014 — **Undergraduate Research Assistant**
Vertical Lift Research Center of Excellence,
The Pennsylvania State University

Teaching Experience

May-June 2016 **International Teaching Assistant**
ENGR 118: Impact of Culture on Engineering in China,
The Pennsylvania State University

June 2014-May 2015 **Teaching Assistant**
EDSGN 497K: Advanced CAD, CATIA
EDSGN 100: Introduction to Engineering Design, Solidworks

Research Interests

Computational Fluid Dynamics
RANS/BEM approaches for optimization of multicopter aircraft
Mixing-plane boundaries in hover cases for reduction in computational cost

Experimental Wind Tunnel Testing

Small-Scale Wind Energy
Blade and rotor design
Electronic control of active pitch system
Systems integration of aerodynamic, mechanical, electrical, and control components

Awards and Honors

Fall 2018 **National Science Foundation Graduate Research Fellowship Program**

Spring 2018 **AHS Vertical Flight Foundation Bell Helicopter Scholarship**

Jan. 2018 **AHS Robert L. Lichten Mid-East Regional Competition Winner**

Fall 2017 **Foreign Language and Area Studies (FLAS) Fellowship**

Spring 2018 **Miller-Arm Endowment**

Spring 2018 **Penn State College of Engineering International Travel Grant**

Spring 2018 **Penn State Education Abroad Whole World Scholarship**

Spring 2018 **The Pennsylvania State University CIEE Scholarship**

Spring 2018 **CIEE Global Access Initiative**

Fall 2017 **Penn State Engineering Alumni Society Scholarship**

Spring 2017 **Goldwater Scholarship Honorable Mention**

Spring 2017 **US Naval Academy Leadership Conference: Schreyer Honors College Representative**

Spring 2017 **College of Engineering Research Initiative (CERI) Student**

Fall 2016 **Penn State Susson Trustee Scholarship**

Fall 2017 **Phi Kappa Psi Foundation District Scholarship**

Fall 2016 **AHS Vertical Flight Foundation Eugene K. Liberatore Scholarship**

Fall 2016 **NASA Pennsylvania Space Grant Undergraduate Scholarship**

Fall 2016 **Penn State Engineering Alumni Society Scholarship**

Fall 2016 **Phi Kappa Psi Foundation Jerry Nelson Award**

Fall 2016 **Phi Kappa Psi Foundation District Scholarship**

Spring 2016 **Sigma Gamma Tau National Aerospace Engineering Honor Society Inductee**

Fall 2015 **Department of Aerospace Engineering Lou Borges Scholarship**

Fall 2015 **Tau Beta Pi National Engineering Honor Society Inductee**

Fall 2014 **Boeing Company Scholarship**

Summer 2014 **Penn State College of Engineering International Travel Grant**

Fall 2013 **Penn State College of Engineering White Trustee Scholarship**

Fall 2013 **The President's Freshman Award**

Fall 2012 **Mountain Top Martial Arts Rank of Shodan (Black Belt)**

Professional Memberships

American Helicopter Society (AHS), member since 2013

American Institute of Aeronautics and Astronautics (AIAA), member since 2014

Organizations and Prior Roles

Wind Energy Club – Founder

Collegiate Wind Competition Team Lead/Aerodynamics Lead

Penn State American Helicopter Society (AHS) – Vice-President

Phi Kappa Psi Fraternity – Pledge Class President/ Academic Chair

Design Build Fly Team Lead

Skills

Aerospace Specific Skills

STAR-CCM+, RotCFD, MATLAB, Linux, ANSYS-FEA/FENSAP, FieldView, Tecplot, XFoil, X-Turb, WT_Perf, CATIA, SolidWorks, BEMT-Design, ICEM, 3D-Printing, Soldering, Electronics

Language and International Experience

Russian ACTFL - Advanced Mid Rating
ILR - Limited Working Proficiency
Intensive Russian Language Program, St. Petersburg State University. St. Petersburg, Russia Spring 2018

Chinese Study Abroad Program, ENGR 118: Impact of Culture on Engineering in China
The Pennsylvania State University, Summers 2014 and 2016

Spanish High School Language Classes

AAUS Science Diving (SCUBA)

Diving Certifications: NAUI Advanced, Rescue, Nitrox, Deep; PADI Open Water

Red Cross CPR, AED, and First Aid; DAN Diving First Aid for Professional Divers

Portfolio: https://drive.google.com/file/d/0Bygpc4Aqwr2SaVZXMnBFR1czZGc/view

LinkedIn: https://www.linkedin.com/in/jason-k-cornelius